

Resveratrol Derivatives from *Vatica albiramis*

Naohito ABE,^a Tetsuro ITO,^a Masayoshi OYAMA,^a Ryuichi SAWA,^b Yoshikazu TAKAHASHI,^b and Munekazu INUMA^{*a}

^aLaboratory of Pharmacognosy, Gifu Pharmaceutical University; 1–25–4 Daigaku-nishi, Gifu, Gifu 501–1196, Japan; and

^bInstitute of Microbial Chemistry; 3–14–23 Kamiosaki, Shinagawa-ku, Tokyo 141–0021, Japan.

Received December 3, 2010; accepted January 10, 2011; published online January 13, 2011

Three new stilbene derivatives, albiraminols A (**1**) (resveratrol hexamer), B (**2**) (resveratrol dimer), and vatalbinoside F (**3**) (mono-glucoside of resveratrol dimer), along with malibatol were isolated from acetone soluble portions of the stem of *Vatica albiramis*. The structures of the isolates were established on the basis of spectroscopic analyses, including a detailed NMR spectroscopic investigation. The biosynthetic aspects of the isolates are discussed in this paper. Compound **1** is composed of tetrameric resveratrol (vaticanol B (1A)) and dimeric resveratrol (1B) and is the first instance of the resveratrol derivative bearing a 5,6,11,12-tetrahydro-5,11-epoxy-dibenzo[*a,e*][8]annulene ring system. Compound **2** possesses a novel 4,5-dihydro-13-oxabenz[3,4]azuleno[7,8,1-*jk*]phenanthrene skeleton in the framework.

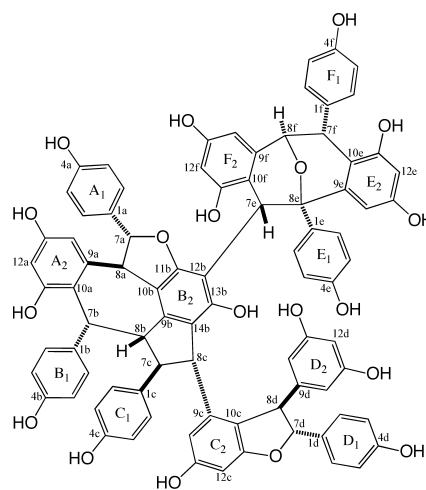
Key words *Vatica albiramis*; Dipterocarpaceae; resveratrol oligomer; structure elucidation; albiraminol

Dipterocarpaceae plants are rich in stilbene oligomers that have a blocking unit of resveratrol.^{1,2)} In recent years, researchers have reported that bioactivities of resveratrol oligomers enable antimicrobial^{3,4)} and antitumor activities,^{5–7)} and enhance regulatory abilities of endoplasmic reticulum stress⁸⁾ and activation abilities of peroxisome proliferator-activated receptors (PPARs).⁹⁾ In our previous studies of the chemical constituents of the stem of *Vatica albiramis* (*V. albiramis*), some new structures of resveratrol oligomers; skeletal variations of the isolates; and the strong inhibitory effect of metalloprotease-1 (MMP-1) production by three major resveratrol tetramers, ((–)-hopeaphenol, vaticanol C, and stenophyllol C were characterized.¹⁰⁾ A further detailed examination of the components in the acetone extract resulted in the isolation of a new resveratrol hexamer, albiraminol A (**1**), and two new resveratrol dimers, albiraminol B (**2**) and vatalbinoside F (**3**).

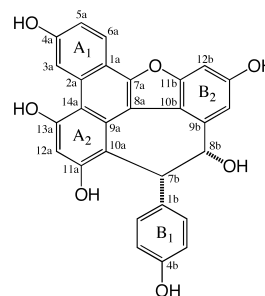
Results and Discussion

An acetone extract of the stem of *V. albiramis* was subjected to column chromatography (CC) on silica gel.¹⁰⁾ To achieve isolation of **1**–**3** along with malibatol, further purification was performed using Sephadex LH-20 CC, reversed-phase CC under medium pressure, and preparative TLC.

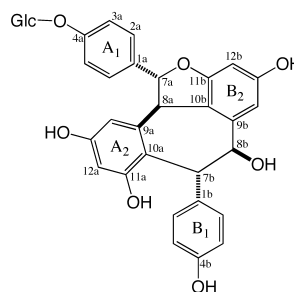
Albiraminol A (**1**),¹¹⁾ obtained as a pale yellow amorphous solid, is the fifth instance of resveratrol hexamers found in nature.^{12,13)} The structure is composed of a tetrameric unit (1A) and a dimeric unit (1B). The former consists of resveratrols A–D ((resveratrol A: ring A₁-7a-8a-ring A₂)), and the latter consists of resveratrols E–H. A detailed structural elucidation was conducted as follows: The molecular formula (C₈₄H₆₂O₁₉), corresponding to a resveratrol hexamer, was deduced from the pseudo-molecular ion [M–H][–] at *m/z* 1375.3951 (Calcd 1375.3958) in the negative ion high resolution-electrospray ionization-mass spectra (HR-ESI-MS). NMR data of **1** was analyzed in the same manner as that of the resveratrol pentamers (upunoside A and hopeasides A and B). The partial structures (1A and 1B) and the connection (C-12b–C-7e) were confirmed by the analysis of the ¹H- and ¹³C-NMR signals (Table 1) supported by double-quantum-filtered correlation spectroscopy (DQF-COSY),



1 ^{a)}



2 ^{a)}



3 ^{b)}

^{a)} relative structure
^{b)} absolute structure

* To whom correspondence should be addressed. e-mail: inuma@gifu-pu.ac.jp

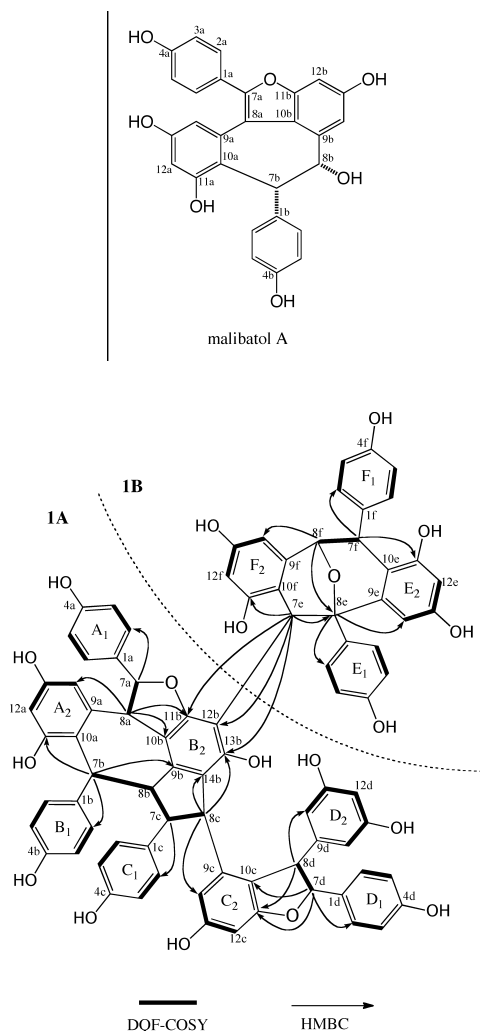


Fig. 1. Selected Correlations in 2D-NMR for Partial Structures (**1A** and **1B**) of **1**

heteronuclear multiple-quantum coherence (HMQC) spectra, and heteronuclear multiple-bond correlation (HMBC) spectra (Fig. 1). The ambiguity of ^1H - and ^{13}C -NMR signals obtained under particular conditions required various conditional NMR measurements. At room temperature, although many proton signals of hydroxy groups were observed, most of them were unclear. On the other hand, clear signals were observed at lower temperatures. Hence, we performed detailed NMR spectral analyses at $-40\text{ }^\circ\text{C}$.

^1H -NMR and DQF-COSY spectral data indicated the presence of six 4-hydroxyphenyl groups (A_1 – F_1); one 3,5-dihydroxyphenyl group (D_2); four 3,5-dioxygenated-1,2-disubstituted benzene rings (A_2 , C_2 , E_2 , and F_2); three mutually coupled aliphatic methine sequences ($\text{CH}(7\text{a})$ – $\text{CH}(8\text{a})$, $\text{CH}(7\text{d})$ – $\text{CH}(8\text{d})$, and $\text{CH}(7\text{f})$ – $\text{CH}(8\text{f})$); and four aliphatic methine sequences successively coupled in the order ($\text{CH}(7\text{b})$ – $\text{CH}(8\text{b})$ – $\text{CH}(7\text{c})$ – $\text{CH}(8\text{c})$) (Fig. 1). NMR data also displayed a methine unit ($\text{CH}(7\text{e})$) and an oxygenated quaternary aliphatic carbon ($\text{C}(8\text{e})$). Among the methine signals, three protons ($\text{H}-7\text{a}$, $\text{H}-7\text{d}$, and $\text{H}-8\text{f}$) were correlated to the oxygen-substituted carbons (δ_{C} 90.7 ($\text{C}-7\text{a}$), 94.3 ($\text{C}-7\text{d}$), and 81.9 ($\text{C}-8\text{e}$)) in the HMQC spectrum. The remaining six quaternary aromatic carbons in the ^{13}C -NMR spectrum ($\text{C}-9\text{b}$ – $\text{C}-14\text{b}$) were assigned to those of the 3,5-dioxygenated, fully substi-

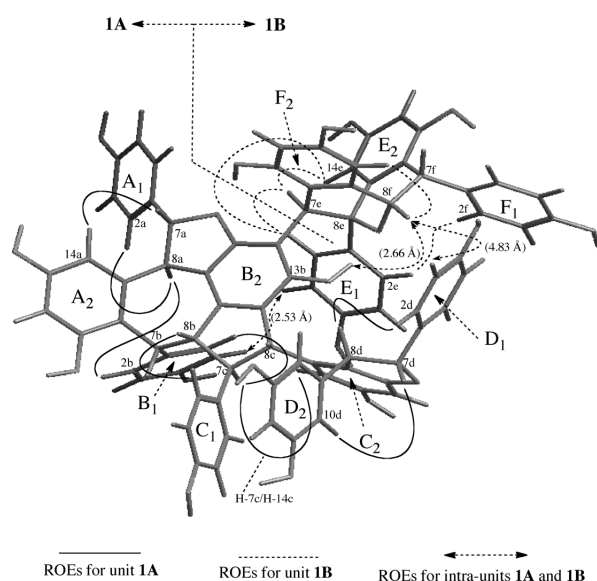


Fig. 2. Selected ROESY Correlations for **1**

Calculated distances of protons for intra-units (**1A** and **1B**) are given in parentheses. The molecule is minimized by MMFF94 calculation using PCMODEL 9.1 molecular modeling program.¹⁴⁾

tuted benzene ring (B_2). The connection of the partial structures in **1A** was established by the HMBC correlations observed between $\text{H}-7\text{a}/\text{C}-2\text{a}(6\text{a})$, $\text{H}-8\text{a}/\text{C}-10\text{b}$, $\text{H}-8\text{a}/\text{C}-14\text{a}$, $\text{H}-7\text{b}/\text{C}-2\text{b}(6\text{b})$, $\text{H}-7\text{b}/\text{C}-9\text{b}$, $\text{H}-8\text{b}/\text{C}-9\text{b}$, $\text{H}-7\text{c}/\text{C}-2\text{c}(6\text{c})$, $\text{H}-8\text{c}/\text{C}-14\text{b}$, $\text{H}-8\text{c}/\text{C}-14\text{c}$, $\text{H}-7\text{d}/\text{C}-2\text{d}(6\text{d})$, $\text{H}-8\text{d}/\text{C}-11\text{c}$, $\text{H}-8\text{d}/\text{C}-10\text{d}(14\text{d})$, and $\text{H}-7\text{d}/\text{C}-11\text{c}$, which indicated 12 C–C bonds and an ether linkage: $\text{C}-1\text{a}-\text{C}-7\text{a}$, $\text{C}-8\text{a}-\text{C}-10\text{b}$, $\text{C}-8\text{a}-\text{C}-9\text{a}$, $\text{C}-1\text{b}-\text{C}-7\text{b}$, $\text{C}-10\text{a}-\text{C}-7\text{b}$, $\text{C}-8\text{b}-\text{C}-9\text{b}$, $\text{C}-1\text{c}-\text{C}-7\text{c}$, $\text{C}-14\text{b}-\text{C}-8\text{c}$, $\text{C}-8\text{c}-\text{C}-9\text{c}$, $\text{C}-1\text{d}-\text{C}-7\text{d}$, $\text{C}-10\text{c}-\text{C}-8\text{d}$, $\text{C}-8\text{d}-\text{C}-9\text{d}$, and $\text{C}-11\text{c}-\text{O}-\text{C}-7\text{d}$. Although another ether linkage ($\text{C}-7\text{a}-\text{O}-\text{C}-11\text{b}$) that forms a hexahydro-benz[5,6]azuleno[7,8,1-*cde*]-benzofuran system was not established because of a lack of a key HMBC, the partial structure **1A** was deduced after considering the molecular formula. The other unit **1B** and the connection of **1A** and **1B** were also deduced by the HMBC correlations that established eight C–C bonds and an ether linkage: $\text{C}-1\text{e}-\text{C}-8\text{e}$, $\text{C}-7\text{e}-\text{C}-8\text{e}$, $\text{C}-7\text{e}-\text{C}-10\text{f}$, $\text{C}-8\text{e}-\text{C}-9\text{e}$, $\text{C}-1\text{f}-\text{C}-7\text{f}$, $\text{C}-7\text{f}-\text{C}-10\text{e}$, $\text{C}-8\text{f}-\text{C}-9\text{f}$, $\text{C}-12\text{b}-\text{C}-7\text{e}$, and $\text{C}-8\text{e}-\text{O}-\text{C}-8\text{f}$.

The relative configuration of **1** was determined by rotating frame Overhauser enhancement spectroscopy (ROESY) experiments and by analyzing the coupling constants using computer-aided molecular modeling (Fig. 2).¹⁴⁾ By the same arguments as those discussed for upunoside A, the structure of **1A** was elucidated as vaticanol B. The relative configuration of **1B** was determined as follows: Considering the framework of the oxabicyclo ring system, ring E_1 and $\text{H}-8\text{f}$ should be located on the same side of the reference plane (α -configuration). The co-facial orientation of the rings E_1 and F_1 was confirmed by the ROE ($\text{H}-2\text{e}(6\text{e})/\text{H}-2\text{f}(6\text{f})$). The β -orientation of $\text{H}-7\text{e}$ was evidenced by the ROE ($\text{H}-7\text{e}/\text{H}-14\text{e}$) as well. The inter-units' ROE was observed for $\text{OH}-13\text{b}$ (**1A**)/ $\text{H}-8\text{f}$ (**1B**), and the distance between them was calculated as 2.66 Å, indicating rotational restriction of the bond $\text{C}-12\text{b}-\text{C}-7\text{e}$. The other ROEs $\text{H}-3\text{b}(5\text{b})$ (**1A**)/ $\text{H}-3\text{e}(5\text{e})$ (**1B**) and $\text{H}-3\text{d}(5\text{d})$ (**1A**)/ $\text{H}-8\text{f}$ (**1B**) indicated the relationship between **1A** and **1B** as shown in Fig. 2 and confirmed the lack

Table 1. 1D- and 2D-NMR Spectral Data of Albiraminol A (1)

No.	25 °C		−40 °C			
	δ_H	δ_C	δ_H	δ_C	HMBC	ROESY
1a		131.4		131.7		
2a(6a)	7.55 (d, 8.8)	130.4	7.50 (d, 8.0)	130.2	3a(5a)*, 4a, 6a(2a), 7a	7a, 8a, 2f(6f)*
3a(5a)	6.84 (d, 8.8)	116.3	6.92 (d, 8.0)	116.0	1a, 4a, 5a(3a)	
4a		158.7	9.11 (br s)	158.37 ^{b)}	3a(5a), 4a	
7a	5.90 (d, 11.8)	90.7	5.85 (d, 12.0)	89.9	2a(6a), 8a*, 9a	2a(6a), 14a
8a	4.59 (d, 11.8)	50.3	4.53 (d, 12.0)	50.9	1a, 7a, 9a, 10b	2a(6a), 2b(6b)
9a		141.8		141.8 ^{f)}		
10a		124.6 ^{h)}		123.7 ^{g)}		
11a		156.7 ⁱ⁾	8.55 (s)	155.4	10a, 11a, 12a	12a
12a	6.25 (br s)	101.4	6.20 ^{e)} (br s)	100.8	14a	11a(OH), 13a(OH)
13a		156.6 ^{j)}	8.51 (s)	156.3	12a, 13a, 14a	12a, 14a
14a	6.20 (br s)	105.3	6.22 (br s)	104.6	8a, 10a, 13a	13a(OH)
1b		133.4		132.9		
2b(6b)	7.01 (d, 8.4)	130.9	6.93 (d, 8.0)	130.6	4b, 6b(2b), 7b	8a, 8b, 7c
3b(5b)	6.78 (d, 8.4)	115.6 ^{j)}	6.72 (d, 8.0)	115.2	1b, 4b, 5b(3b)	
4b		155.8	8.71 (s)	155.5	3b(5b), 4b	
7b	5.06 ^{o)} (d, 5.2)	37.0	4.97 (d, 2.0)	36.4	9a, 10a, 11a, 1b, 2b(6b), 8b, 9b	2b(6b)
8b	2.90 ⁿ⁾ (br d)	52.7	2.87 (br d, 10.0)	52.4	1b, 7b, 9b, 7c*	
9b		141.8		140.3		
10b		113.6		113.3		
11b		155.6		157.0		
12b		110.2		110.2		
13b		153.1	8.72 (s)	152.8	12b, 13b, 14b	8f
14b		124.6 ^{h)}		123.7 ^{g)}		
1c		131.6		131.0		
2c(6c)	6.27 (d, 8.8)	129.1	6.16 (d, 8.0)	128.8	3c(5c)*, 4c, 6c(2c), 7c	7c, 8c
3c(5c)	6.39 (d, 8.8)	115.7 ^{j)}	6.33 (d, 8.0)	115.2	1c, 4c, 5c(3c)	4c(OH)
4c		156.0 ^{e)}	8.25 (s)	155.7 ^{l)}	3c(5c), 4c	3c(5c)
7c	3.77 (dd, 12.0, 11.0)	58.2	3.68 (dd, 10.0)	58.1	7b, 1c, 2c(6c), 9c	2c(6c)
8c	4.20 (d, 11.0)	49.8	4.19 (d, 10.0)	48.9	14b, 1c, 7c, 9c, 14c	2c(6c)
9c		142.2		141.8 ^{f)}		
10c		123.2		122.8		
11c		160.7		160.1		
12c	5.97 ^{b)} (br s)	95.2	5.81 (br like d)	94.7	10c, 11c, 13c, 14c	13c(OH)
13c		158.5	8.27 (s)	158.41 ^{k)}	12c, 13c, 14c	12c, 14c
14c	5.97 ^{b)} (br s)	107.0	5.90 (br s)	106.3	8c, 10c, 12c, 13c	7c
1d		134.8		133.8		
2d(6d)	7.08 (d, 8.4)	128.1	7.14 (d, 8.0)	128.6	3d(5d), 4d, 6d(2d), 7d	7d, 8d
3d(5d)	6.86 (d, 8.4)	115.9	6.95 (d, 8.0)	115.6	1d, 4d, 5d(3d)	8f*
4d		157.7		157.8		
7d	5.19 (d, 4.6)	94.3	5.14 (d, 4.0)	94.0	11c, 2d(6d), 9d	2d(6d), 10d, 14d
8d	4.39 (d, 4.6)	56.6	4.41 (d, 4.0)	55.4	10c, 11c, 1d, 9d, 10d, 14d	2d(6d), 10d, 14d
9d		148.5		148.5		
10d	5.89 (br s)	107.3	5.61 (br s)	106.1	8d*, 12d, 14d	7d, 8d
11d		159.5	8.44 (br s)	158.6	11d	
12d	6.15 (t, 2.0)	101.8	6.14 (br like t)	101.3	10d, 11d, 13d, 14d	
13d		159.5	8.19 (s)	160.0	12d, 13d	
14d	5.89 (br s)	107.3	6.07 (br s)	107.5	8d*, 10d, 12d	7d, 8d
1e		138.5		135.0		
2e(6e)	7.55 (d, 8.8)	128.5	7.61 (d, 8.0)	128.2	4e, 6e(1e), 8e	7e, 14e, 2f(6f)
3e(5e)	6.84 (d, 8.8)	114.9	6.85 (d, 8.0)	114.4	1e, 4e, 5e(3e)	
4e		156.9		156.8 ^{m)}		
7e	5.05 ^{o)} (s)	43.1	5.13 (s)	42.7	11b, 12b, 13b, 8e, 9e, 9f, 10f	2e(6e), 14e, 11f
8e		81.9		82.1		
9e		143.1 ^{d)}		143.2		
10e		112.8		112.0		
11e		156.0 ^{c)}	8.54 (s)	155.8 ^{l)}	10e, 11e, 12e	12e
12e	6.14 (d, 2.0)	102.2	6.11 (d, 2.0)	101.4	10e, 13e, 14e	11e(OH), 13e(OH)
13e		157.1	8.43 (s)	156.8	12e, 13e, 14e	12e, 14e
14e	6.50 (d, 2.0)	105.0	6.22 (br s)	104.7	8e, 10e, 12e, 13e	2e(6e), 7e, 13e(OH)
1f		135.9		135.6		
2f(6f)	6.85 (d, 8.4)	130.7	7.21 (d, 8.0)	130.3	3f(5f)*, 4f, 6f(2f), 7f	2a(6a)*, 2c(6c), 7f, 8f
3f(5f)	7.25 (d, 8.4)	115.5 ^{j)}	6.78 (d, 8.0)	115.3	1f, 4f, 5f(3f)	4f(OH)
4f		156.8	8.62 (s)	156.5	3f(5f), 4f	3f(5f)
7f	4.36 (s)	46.5	4.37 (br s)	46.0	9e, 10e, 11e, 1f, 2f(6f)	2f(6f), 14f
8f	5.35 (s)	79.4	5.33 (br s)	79.2	8e, 10e, 1f, 7f, 9f, 14f	13b(OH), 3d(5d)*, 2f(6f), 14f
9f		143.1 ^{d)}		138.2		
10f		112.9		112.9		
11f		156.4	8.35 (s)	156.7 ^{m)}	10f, 11f, 12f	7e, 12f
12f	6.19 (d, 2.4)	102.9	6.20 ^{e)} (br s)	102.3	10f, 14f	13b(OH)
13f		157.3		157.0		
14f	6.57 (d, 2.4)	103.8	6.65 (br s)	102.9	8f, 10f, 12f, 13f	7f, 8f

Values are in ppm (δ_H and δ_C). Measured in acetone- d_6 at 600 MHz ($^1\text{H-NMR}$) and 125 MHz ($^{13}\text{C-NMR}$). All protons and carbons were assigned from DQF-COSY, HMQC and HMBC spectra. *a–g*) Overlapping; *h–m*) interchangeable; *n*) masked by H_2O signal; * weak correlations.

of an enantiomeric structure of **1B**. The distances between the ROEs H-3b(5b) (**1A**)/H-3e(5e) (**1B**) and H-3d(5d) (**1A**)/H-8f were calculated as 2.66 Å and 4.83 Å, respectively. Therefore, albiraminol A (**1**) was elucidated as $\{(3S^*,4S^*,4aR^*,5R^*,9bR^*,10R^*)-1-[(5R^*,6S^*,11S^*,12S^*)-1,3,7,9\text{-tetrahydro-5,12-bis(4-hydroxyphenyl)-5,6,11,12-tetrahydro-5,11-epoxydibenzo}[a,e][8]\text{annulene-6-yl}]-3-[(2R^*,3R^*)-3-(3,5\text{-dihydroxyphenyl})-2,3\text{-dihydro-6-hydroxy-2-(4-hydroxyphenyl)benzofuran-4-yl}]-3,4,4a,5,9b,10\text{-hexahydro-4,5,10-tris(4-hydroxyphenyl)benz}[5,6]\text{azuleno-}[7,8,1-cde]\text{-benzofuran-2,6,8-triol}\}$.

The blocking units of **1** were six resveratrols A–F, among which resveratrol F possessed the rearranged aromatic ring (ring H₁) that resulted from the 1,2-aryl shift. The 1,2-aryl shift products of the resveratrol oligomers have rarely been isolated, and examples of isolation include two trimers, cotylelophenol A¹⁵⁾ and grandiphenol D.¹⁶⁾ Compound **1** can be considered to be a condensed product of resveratrol tetramer (**1A**: vaticanol B) and resveratrol dimer (**1B**). As previously discussed, vaticanol B, one of the major constituents, functions as a blocking unit in the biogenesis of highly condensed resveratrol oligomers as elucidated by structures of vaticanol J (heptamer),¹²⁾ upunoside A (pentamer),¹⁷⁾ and pauciflorol D (heptamer),¹⁸⁾ and can be applicable to the biosynthetic pathway of **1**. Compound **1** is the first example of resveratrol hexamers bearing the blocking unit of vaticanol B.

Albiraminol B (**2**),¹¹⁾ obtained as a pale yellow amorphous solid, demonstrated a positive Gibbs reaction. The composition of **2** was deduced to be C₂₈H₁₈O₇ from the pseudo-molecular ion peak $[M-H]^-$ at m/z 465.0974 in the HR-FAB-MS (negative ion mode), which indicated that **2** was an oxidative product of a resveratrol dimer. ¹H- and ¹³C-NMR data analyzed using DQF-COSY, HMQC, and HMBC spectra revealed the presence of a 1,2,4-trisubstituted benzene ring (A₁), 4-oxygenated phenyl group (B₁), 3,5-dioxygenated-1,2,6-trisubstituted benzene ring (A₂), and 3,5-dioxygenated-1,2-trisubstituted benzene ring (B₂). The data also showed the presence of one mutually coupled aliphatic methine (CH(7b)–CH(8b)) and two quaternary olefinic carbons (C-7a and C-8a) of which C-8b (δ_C 74.4) and C-7a (δ_C 151.6) were attached to oxygen (Fig. 3, Table 2). An alcoholic hydroxy group (δ_H 5.08) was also observed in the ¹H-NMR spectrum. These partial structures were connected as **2A** by the HMBC correlations, revealing the C–C bonds between C-1a–C-7a, C-1b–C-7b, C-8b–C-9b, C-7b–C-10a, and C-2a–C-14a (**2A**). The proposed partial structures of the four aromatic rings in **2A** accounted for 16 out of 20 degrees of unsaturation, which indicated that **2** required three additional ring formations, including an ether linkage and an olefinic bond (C-7a–C-8a). The consequent skeleton was a 4,5-dihydro-13-oxabenzofuran ring. The comparison of spectral data in the benzofuran moiety with those of malibatol A supported the connections (C-7a–C-8a, C-8a–C-9a, and C-8a–C-10b, and C-7a–O–C-11b). The other six oxygen atoms were in hydroxy groups given the molecular formula. The relative configuration and conformation of **2** were determined by analysis of the coupling constants by using computer-aided molecular modeling. Two relative configurations **2B** (7b*R**,8b*R**) and **2C** (7b*R**,8b*S**) were proposed for **2**. The minimum energy con-

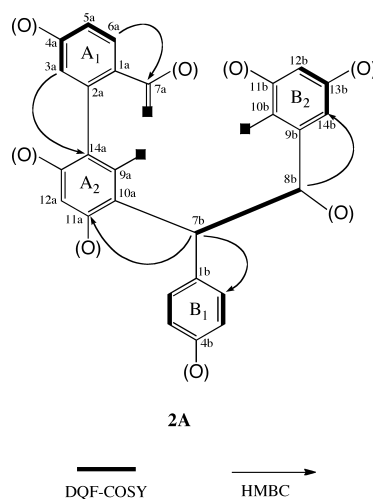


Fig. 3. Selected Correlations in 2D-NMR for Partial Structure (**2A**) of **2**

Table 2. 1D- and 2D-NMR Spectral Data of Malibatol A and Albiraminol B (**2**)

No.	Malibatol A [†]		Albiraminol B (2) [‡]		
	δ_H	δ_C	δ_H	δ_C	HMBC
1a		124.4		115.1	
2a	7.54 (d, 8.8)	130.8	8.21 (d, 8.8)	121.9	1a, 4a, 7a
3a	6.92 (d, 8.8)	116.4	7.23 (dd, 8.8, 2.4)	115.6	1a
4a		158.6		156.8	
5a	6.92 (d, 8.8)	116.4	9.41 (d, 2.4)	114.5	1a, 4a, 14a
6a	7.54 (d, 8.8)	130.8		133.7 ^{a)}	
7a		150.8		151.6	
8a		117.1		114.8	
9a		135.6		133.7 ^{a)}	
10a		120.5		116.1	
11a		157.0		155.0	
12a	6.49 (d, 2.4)	102.4	6.95 (s)	102.3	9a, ^{c)} 10a, 13a, 14a, 5b ^{c)}
13a		156.7		157.2	
14a	6.66 (d, 2.4)	109.7		112.0	
1b		133.0		133.4	
2b(6b)	7.20 (d, 8.6)	130.4	6.87 (d, 8.8)	130.9	4b, 6b(2b), 7b
3b(5b)	6.45 (d, 8.6)	114.8	6.31 (d, 8.8)	114.7	1b, 4b, 5b(3b)
4b		155.5		155.8	
7b	5.59 (br s)	48.4	5.87 (br s)	49.0	9a, 10a, 11a, 6b(2b), 8b
8b	5.43 (br s)	74.4	5.56 (br s)	74.4	
9b		139.7		139.6	
10b		118.5		115.9	
11b		154.7		157.5 ^{b)}	
12b	6.67 (d, 2.0)	95.9	6.92 (s)	96.4	10b, 11b, 13b, ^{d)} 14b ^{d)}
13b		156.1		156.3 ^{b)}	
14b	7.22 (d, 2.0)	110.2	7.15 (s)	109.5	8b, 10b, 12b
8b(OH)			5.08 (br s)		

Values are in ppm (δ_H and δ_C). [†] Measured in acetone-*d*₆ at 300 MHz (¹H-NMR) and 75 MHz (¹³C-NMR). [‡] Measured in acetone-*d*₆ at 400 MHz (¹H-NMR) and 100 MHz (¹³C-NMR). All protons and carbons were assigned from DQF-COSY, HMQC and HMBC spectra. a) Overlapping, b) interchangeable, c) 4J, d) undistinguishable.

formations of each conformer were obtained using the PC-MODEL with the Merck molecular force field (MMFF94) (Fig. 4). According to the results, the energy-minimized conformations displayed a dihedral angle of 76.9° for **2B** and 45.9° for **2C**. **2B** only explained the small coupling constant for H-7b/H-8b (Table 2), and no NOE observation for H-2b(6b)/H-8b. Therefore, the structure of albiraminol B (**2**) was elucidated as (4*R**,5*R**)-5-(4-hydroxyphenyl)-4,5-dihy-

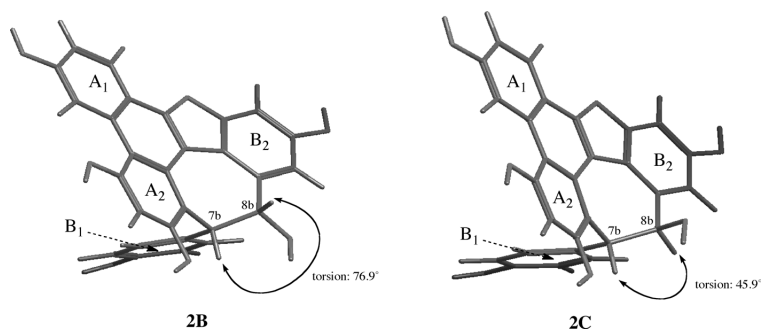


Fig. 4. Two Possible Configurations (**2B** and **2C**) for **2** and Dihedral Angles for H-7b and H-8b

Each configuration is minimized by MMFF94 calculation using PCMODEL 9.1 software.¹⁴⁾

Table 3. 1D- and 2D-NMR Spectral Data of (–)-Ampelopsin A and Vatalbinoside F (**3**)

No.	(–)-Ampelopsin A [†]		Vatalbinoside F (3) [‡]		
	δ_{H}	δ_{C}	δ_{H}	δ_{C}	HMBC
1a		132.5		134.4	
2a(6a)	7.09 (d, 8.3)	129.9	7.14 (d, 8.8)	130.0	4a, 6a(2a), 7a
3a(5a)	6.75 (d, 8.3)	116.0	7.02 (d, 8.8)	117.6	1a, 5a(3a)
4a		158.4 ^{d)}		156.2	
7a	5.42 (d, 11.3)	88.3	5.75 (d, 11.5)	88.7	2a(6a), 9a
8a	4.15 (br d, 11.3)	49.5	4.02 (d, 11.5)	50.3	1a, 9a, 10b
9a		143.1		143.3	
10a		118.2		119.1	
11a		157.2		159.2 ^{b)}	
12a	6.42 (d, 2.5)	101.6	6.32 (d, 2.0)	101.6	10a, 11a, 13a, 14a
13a		158.8 ^{c)}		157.5	
14a	6.21 (br s)	105.5	6.13 ^{d)} (d, 2.0)	105.3	10a, 12a, 13a
1b		130.9		133.1	
2b(6b)	6.88 (d, 8.3)	128.7	6.82 (d, 8.8)	129.0	4b, 6b(2b), 7b
3b(5b)	6.62 (d, 8.3)	115.4	6.57 (d, 8.8)	115.7	1b, 5b(3b)
4b		156.0 ^{d)}		159.3	
7b	5.45 (d, 4.9)	43.8	5.38 (br s)	44.1	9a, 10a, 11b, 1b, 2b(6b)
8b	5.42 (br d, 4.9)	71.2	5.38 (br s)	71.7	9b, 10b, 14b
9b		140.2		139.8	
10b		118.9		119.7	
11b		160.1		159.4 ^{b)}	
12b	6.14 (br d, 1.9)	97.1	6.13 ^{d)} (d, 2.0)	97.6	10b, 11b, 13b, 14b
13b		158.8 ^{c)}		160.5	
14b	6.64 (d, 1.9)	110.5	6.54 (d, 2.0)	110.9	8b, 10b, 12b, 13b
glc-1			4.90 (d, 7.3)	102.1	
glc-2			3.43 (m)	74.9	4a
glc-3			3.41 (m)	78.1	
glc-4			3.36 (m)	71.4	
glc-5			3.45 (m)	78.0	
glc-6			3.93 (d, 12.2)	62.5	
			3.68 (dd, 12.2, 5.4)		

Values are in ppm (δ_{H} and δ_{C}). Measured in [†]acetone-*d*₆ and [‡]methanol-*d*₄ at 400 MHz (¹H-NMR) and 100 MHz (¹³C-NMR). All protons and carbons were assigned from DQF-COSY, HMQC and HMBC spectra. *a, b*) Interchangeable; *c, d*) overlapping.

dro-13-oxabenz[3,4]azuleno[7,8,1-*ijkl*]phenanthrene-2,4,6,8,10-pentaol. Compound **2** bore the same configuration of two methines as that of malibatol, indicating that **2** was produced following the dehydrogenation of malibatol.

Two resveratrol units produced various heterocyclic ring systems in plants represented by dihydrobenzofuran, bicyclo[3.2.1]octadiene, bicyclo[5.3.0]decadiene, and bicyclo[3.3.0]octadiene.¹⁾ The occurrence of a novel skeleton, 4,5-dihydro-13-oxabenz[3,4]azuleno[7,8,1-*ijkl*]phenanthren, demonstrated the diversity of the resveratrol oligomers in

dipterocarpaceous plants.

Vatalbinoside F (**3**) was obtained as a yellow amorphous solid. The composition was deduced to be C₃₄H₃₂O₁₂ from the pseudo-molecular ion peak [M–H][–] at *m/z* 631.1809 in the HR-FAB-MS (negative ion mode). The NMR spectra supported the presence of a β -glucopyranosyloxy group. ¹H- and ¹³C-NMR data of **3** (Table 3), except for the β -glucopyranosyloxy group, showed close similarity to that of ampelopsin A¹⁹⁾ and vatalbinoside E.¹⁰⁾ The HMBC and nuclear Overhauser effect spectroscopy (NOESY) spectra (Table 3) confirmed the relative structure of aglycone (ampelopsin A) and the position of the *O*- β -glucopyranosyloxy group. The circular dichroism (CD) curve of **3** was similar to that of (–)-ampelopsin A. Therefore, the structure of vatalbinoside F (**3**) was elucidated as (–)-ampelopsin A-4a-*O*- β -glucopyranoside.

Experimental

General Experimental Procedures The following instruments were used: optical rotations, JASCO P-1020 polarimeter; UV spectra, Shimadzu UV-3100 spectrophotometer (MeOH solution); CD spectra, JASCO J-820 spectrometer (MeOH solution); ¹H- and ¹³C-NMR spectra, JEOL JNM ECA-600 and JEOL JNM AL-400 (chemical shift values in ¹H-NMR spectra presented as δ values using tetramethylsilane (TMS) as an internal standard); ESI-MS, Thermo Fisher Scientific LTQ Orbitrap instrument; and FAB-MS, JEOL JMS-DX-300 instrument.

The following adsorbents were used for purification: analytical TLC, Merck Kieselgel 60 F₂₅₄ (0.25 mm); preparative TLC, Merck Kieselgel 60 F₂₅₄ (0.5 mm); column chromatography, Merck Kieselgel 60, Pharmacia Fine Chemicals AB Sephadex LH-20 and Fuji Silysia Chemical Chromatorex DMS; and vacuum-liquid chromatography (VLC), Merck Kieselgel 60. A Waters Sep-Pak C₁₈ cartridge was used for small-scale reversed-phase open-column chromatography. The following system was used for preparative HPLC: LC-6AD pump, a SIL-10AXL auto injector, a SCL-10AVP system controller, and a SPD-10AV UV-Vis absorbance detector equipped with CLASS-VP software. The separation was performed on a Capcell Pak C18 UG120 S-5 column (5 mm, 250 mm×10.0 mm; Shiseido, Japan) at 40 °C. The flow rate of the mobile phase was 5 ml/min, and detection was performed at 280 nm.

Plant Material *Vatica albiramis* was collected in Borneo, Malaysia in April 2002, identified by J. Josue, head of the forest product branch of the Forest Research Center, Sandakan Sabah, Malaysia. A voucher specimen number DP-026 was deposited at the herbarium of Gifu Pharmaceutical University.

Extraction and Isolation The extraction and isolation procedures were the same as those in our previous study.¹⁰⁾ Compound **2** (24.0 mg) was obtained from fraction 4 after purification by column chromatography over Sephadex LH-20 (MeOH) and ODS (MeOH/H₂O system). Purification of the ninth fraction using silica gel column chromatography (CHCl₃/MeOH gradient system), Sephadex LH-20 (MeOH), Sep-Pak C₁₈ (MeOH/H₂O system), VLC (EtOAc/CHCl₃/MeOH/H₂O system), reversed phase MPLC (MeOH/H₂O system), and PTLC (EtOAc/CHCl₃/MeOH/H₂O system)

achieved the isolation of compounds **1** (16.7 mg) and **3** (9.0 mg).

Albiraminol A (**1**): A yellowish solid. $^1\text{H-NMR}$ (acetone- d_6 , 600 MHz) and $^{13}\text{C-NMR}$ (acetone- d_6 , 150 MHz); see Table 1. UV λ_{max} (MeOH) nm (log ϵ): 283 (4.48). CD (c 7.2 μM , MeOH) nm ($\Delta\epsilon$) 239 (−9.0). ESI-MS m/z : 1373 [M−H] $^-$; negative ion HR-ESI-MS m/z : 1373.3951 [M−H] $^-$ (Calcd for $\text{C}_{84}\text{H}_{64}\text{O}_{19}$: 1373.3958). $[\alpha]_{\text{D}}^{25}$ −17.8° (c =0.1, MeOH).

Albiraminol B (**2**): A brown solid. $^1\text{H-NMR}$ (acetone- d_6 , 400 MHz) and $^{13}\text{C-NMR}$ (acetone- d_6 , 100 MHz); see Table 2. UV λ_{max} (MeOH) nm (log ϵ): 229 (4.35), 277 (4.18), 336 (3.80). CD (c 21.5 μM , MeOH) nm ($\Delta\epsilon$) 216 (+4.2), 236 (−5.3), 262 (+6.7). FAB-MS m/z : 465 [M−H] $^-$; and negative ion HR-FAB-MS m/z : 465.0979 (M−H) $^-$ (Calcd for $\text{C}_{28}\text{H}_{17}\text{O}_7$: 465.0974). $[\alpha]_{\text{D}}^{25}$ −28.0° (c =0.1, MeOH).

Vatambinose F (**3**): A yellowish solid. $^1\text{H-NMR}$ (acetone- d_6 , 400 MHz) and $^{13}\text{C-NMR}$ (acetone- d_6 , 100 MHz); see Table 3. UV λ_{max} (MeOH) nm (log ϵ): 231 (4.35), 284 (4.18). CD (c 7.2 μM , MeOH) nm ($\Delta\epsilon$) 236 (−9.6). FAB-MS m/z : 631 [M−H] $^-$; and negative ion HR-FAB-MS m/z : 631.1822 (M−H) $^-$ (Calcd for $\text{C}_{34}\text{H}_{31}\text{O}_{12}$: 631.1816). $[\alpha]_{\text{D}}^{25}$ −120.2° (c =0.1, MeOH).

References and Notes

- Ito T., *Yakugaku Zasshi*, **131**, 93—100 (2011).
- Sotheeswaran S., Pasupathy V., *Phytochemistry*, **32**, 1083—1092 (1993).
- Zgoda-Pols J. R., Freyer A. J., Killmer L. B., Porter J. R., *J. Nat. Prod.*, **65**, 1554—1559 (2002).
- Nitta T., Arai T., Takamatsu H., Inatomi Y., Murata H., Iinuma M., Tanaka T., Ito T., Asai F., Iliya I., Nakanishi T., Watabe K., *J. Health Sci.*, **48**, 273—276 (2002).
- Seo E.-K., Chai H., Constant H. L., Santisuk T., Reutrakul V., Beecher C. W. W., Farnsworth N. R., Cordell G. A., Pezzuto J. M., Kinghorn A. D., *J. Org. Chem.*, **64**, 6976—6983 (1999).
- Ito T., Akao Y., Yi H., Ohguchi K., Matsumoto K., Tanaka T., Iinuma M., Nozawa Y., *Carcinogenesis*, **24**, 1489—1497 (2003).
- Shibata M. A., Akao Y., Shibata E., Nozawa Y., Ito T., Mishima S., Morimoto J., Otsuki Y., *Cancer Chemother. Pharmacol.*, **60**, 681—691 (2007).
- Tabata Y., Takano K., Ito T., Iinuma M., Yoshimoto T., Miura H., Kitao Y., Ogawa S., Hori O., *Am. J. Physiol.*, **293**, C411—C418 (2007).
- Tsakamoto T., Nakata R., Tamura E., Kosuge Y., Kariya A., Katsukawa M., Mishima S., Itoh T., Iinuma M., Akao Y., Nozawa Y., Arai Y., Namura S., Inoue H., *Nutr. Metab.*, **7**, No pp given: (<http://www.nutritionandmetabolism.com/content/7/1/46>).
- Abe N., Ito T., Oyama M., Sawa R., Takahashi Y., Iinuma M., “51st Symposium on the Chemistry of Natural Products,” Nagoya, 7—9 October, 2009, Symposium Papers, pp. 551—556.
- Ito T., Tanaka T., Nakaya K. i., Iinuma M., Takahashi Y., Naganawa H., Ohyama M., Nakanishi Y., Bastow K. F., Lee K. H., *Tetrahedron*, **57**, 7309—7321 (2001).
- Ito T., Tanaka T., Ali Z., Akao Y., Nozawa Y., Takahashi Y., Sawa R., Nakaya K., Murata J., Darnaedi D., Iinuma M., *Heterocycles*, **63**, 129—136 (2004).
- PCMODEL v9.0, Serena Software, Box 3076, Bloomington, IN 47402-3076.
- Ito T., Ali Z., Furusawa M., Iliya I., Tanaka T., Nakaya K., Murata J., Darnaedi D., Oyama M., Iinuma M., *Chem. Biodivers.*, **2**, 1200—1216 (2005).
- Ito T., Abe N., Oyama M., Tanaka T., Murata J., Darnaedi D., Iinuma M., *Helv. Chim. Acta*, **92**, 1203—1216 (2009).
- Ito T., Ali Z., Iliya I., Furusawa M., Tanaka T., Nakaya K., Takahashi Y., Sawa R., Murata J., Darnaedi D., Iinuma M., *Helv. Chim. Acta*, **88**, 23—34 (2005).
- Ito T., Tanaka T., Iinuma M., Nakaya K., Takahashi Y., Sawa R., Murata J., Darnaedi D., *J. Nat. Prod.*, **67**, 932—937 (2004).
- Oshima Y., Ueno Y., Hikino H., Ling-Ling Y., Kun-Ying Y., *Tetrahedron*, **46**, 5121—5126 (1990).